Journal of Power Sources 97–98 (2001) 371–376

JOURNAL OF POWER SOURCES

www.elsevier.com/locate/jpowsour

Lithium transport through $Li_{1-\delta}Mn_2O_4$ electrode involving the ordering of lithium ion by numerical analysis of current transient

Su-Il Pyun*, Sung-Woo Kim

Department of Materials Science and Engineering, Korea Advanced Institute of Science and Technology, 373-1 Kusong-Dong, Yusong-Gu, Taejon 305-701, South Korea

Received 6 June 2000; received in revised form 7 November 2000; accepted 11 December 2000

Abstract

Lithium transport through $Li_{1-\delta}Mn_2O_4$ electrode during the lithium intercalation involving the disorder to order phase transition was investigated by numerical analysis of the current transient. All the measured current transients showed non-Cottrell behaviour during the whole lithium intercalation, and the relationship between the initial current level and the applied potential drop followed Ohm's law. The current transient was numerically simulated based upon the 'cell-impedance controlled' lithium transport at various applied potential steps. The current transient theoretically calculated well coincided with that transient experimentally measured in value and shape. The typical current transient showed two 'quasi-current plateaux' separated by a steep current drop in value, indicating the coexistence of the disordered and ordered phases, as confirmed from the concentration profile across the electrode. From the experimental and theoretical results, it was strongly inferred that lithium transport through the $Li_{1-\delta}Mn_2O_4$ electrode is governed by the 'cell-impedance controlled' constraint during the whole lithium intercalation involving the ordering of lithium ion.

Keywords: Lithium manganese oxide; Disorder to order phase transition; Lithium transport; Current transient; Cell-impedance

1. Introduction

Lithium manganese oxide with the cubic-spinel structure is of great interest as intercalation electrode for use in rechargeable lithium batteries, because of its high electrode potential and stability of the crystal structure [1]. It has been reported [1–8] that the disorder to order phase transition occurs during the lithium intercalation into the cubic-spinel lithium manganese oxide, due to the strong repulsive interaction between lithium ions. Besides $LiMn_2O_4$, the disorder to order phase transition was also reported in other intercalation compounds such as $LiTaS_2$ [9] and $LiCoO_2$ [10,11].

Most researches on lithium transport through the cubic-spinel lithium manganese oxide electrode have been focussed on diffusion of lithium ion within the oxide, assuming that diffusion of lithium ion is the rate-controlling process of the lithium intercalation [12]. However, little attention has been paid to the effect of the disorder to order transition during the lithium intercalation on lithium transport in spite of its relevance.

Recently, in our previous works on the analysis of the potentiostatic current transients, it has been reported that lithium transport through the $Li_{1-\delta}CoO_2$ [13,14], $Li_{1+\delta}[Ti_{5/3}Li_{1/3}]O_4$ [15], $Li_{1-\delta}NiO_2$ [15] and $Li_{\delta}V_2O_5$ [15] electrodes is obviously controlled by the 'cell-impedance' under the 'apparent' potentiostatic boundary condition rather than the 'real' potentiostatic boundary condition. In addition, from the appearance of the 'current plateau' in the current transient, it has been suggested that phase transformation of α to β also occurs under the 'cell-impedance controlled' constraint during the lithium intercalation.

In this work, therefore, lithium transport through the $Li_{1-\delta}Mn_2O_4$ electrode involving the disorder to order transition was analysed based upon the 'cell-impedance controlled' constraint. For this purpose, potentiostatic current transients were first measured on the electrode as a function of applied potential. On the basis of the assumption that the lithium intercalation is purely limited by 'cell-impedance', the current transients were then numerically simulated as a function of applied potential and compared with those current transients experimentally measured.

2. Experimental

The carbon-dispersed composite electrode composed of the sol–gel derived $LiMn_2O_4$ powder, 6 wt.% Vulcan XC-72

* Corresponding author. Tel.: +82-42-869-3319; fax: +82-42-869-3310.
E-mail address: sipyun@mail.kaist.ac.kr (S.-I. Pyun).

0378-7753/01/$ – see front matter
PII: S0378-7753(01)00550-X

carbon black and 2 wt.% poly-vinylidene fluoride (PVDF) was prepared as described previously [16]. From inductively coupled plasma (ICP) analysis, the real molar Li/Mn ratio of the sol–gel derived $LiMn_2O_4$ powder was determined to be 0.514, indicating that the oxide is composed of the lithium-excess spinel phase.

A three-electrode electrochemical cell was employed for the electrochemical experiment. Both the reference and counter electrodes were lithium foil (Foote Mineral, USA, purity 99.9%) and a 1 M solution of lithium perchlorate ($LiClO_4$) in propylene carbonate (PC) was used as the electrolyte. All the electrochemical experiments were usually performed at 25°C in a glove box (MECAPLEX GB94) filled with purified argon gas.

Galvanostatic intermittent titration technique (GITT) was employed by using Solartron 1287 electrochemical interface (ECI). Applying a constant current to the cell during 900 s upon discharging,[1] the resulting cell potential transients were recorded. The discharge current was selected so that a change in lithium content of $\Delta\delta = 1$ for $Li_{1-\delta}Mn_2O_4$ would occur over 10 h. The deviation from the ideal stoichiometry of $Li_{1-\delta}Mn_2O_4$, δ, was calculated from the mass of the oxide and the electrical charge that was transferred upon discharging. In order to obtain uniform distribution of lithium ions over the electrode after interruption of the constant current, it required about 1 h to reach equilibrium. After that the open circuit potential was just recorded as an electrode potential.

Potentiostatic current transient technique was performed by application of various large potential steps (0.1–0.45 V). The current transient was measured on the carbon-dispersed composite electrode by dropping 4.25 V_{Li/Li^+} to the lithium injection potential in the range 3.8–4.15 V_{Li/Li^+} for 1×10^4 s. Prior to lithium injection, the electrode was maintained at 4.25 V_{Li/Li^+} for 5×10^3 s to obtain a low steady-state current.

3. Results and discussion

Fig. 1(a) presents the electrode potential E versus lithium content $(1-\delta)$ curve obtained from the cell of Li/1 M $LiClO_4$–PC solution/$Li_{1-\delta}Mn_2O_4$ electrode. As lithium content increased, the electrode potential curve showed a steep potential drop at $(1-\delta) = 0.5$, which is typical of the disorder to order phase transition in the electrode [1–8]. For the thermodynamic second-order transition one can expect that the susceptibility of the system, which is strongly related with the inverse derivative of the electrode potential curve, diverges at the transition points [9,17], and hence we can experimentally determine the stable regions of the disordered and ordered phases as shown in Fig. 1(b).

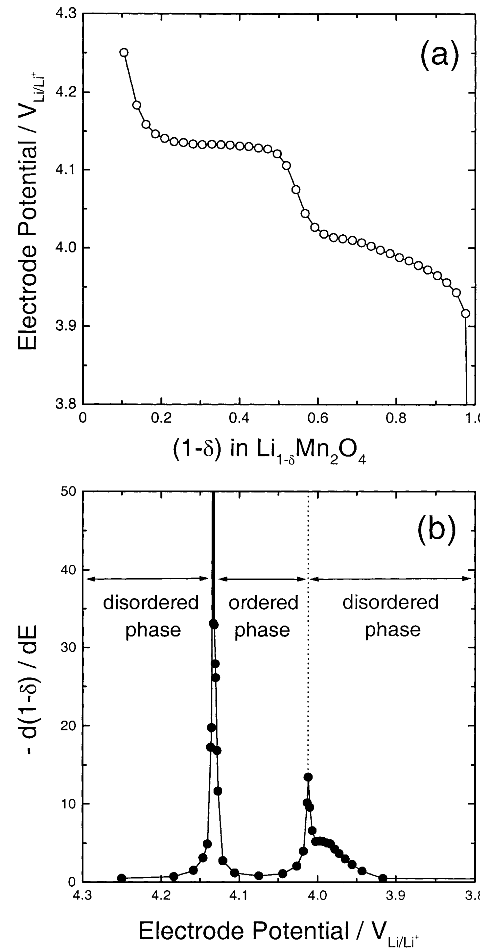

Fig. 1. (a) Electrode potential E vs. lithium content $(1-\delta)$ curve experimentally obtained from the cell of Li/1 M $LiClO_4$–PC solution/ $Li_{1-\delta}Mn_2O_4$ electrode, and (b) the inverse derivative of the electrode potential vs. lithium content curve.

Fig. 1(b) gives the inverse derivative of the electrode potential versus lithium content curve. As the electrode potential decreases with lithium content during the lithium intercalation into the electrode, the disorder to order transition occurs at the first peak (ca. 4.13 V_{Li/Li^+}), and then the order to disorder transition takes place at the second peak (ca. 4.01 V_{Li/Li^+}) of the inverse derivative curve. It is noteworthy that the transition points experimentally obtained were well consistent in value with those transition points determined from the theoretical phase diagram for the disorder to order phase transition in the $Li_{1-\delta}Mn_2O_4$ electrode which was reported in our previous work [8].

Fig. 2(a) shows the cathodic current transients on a logarithmic scale experimentally obtained from the $Li_{1-\delta}$-Mn_2O_4 electrode in a 1 M $LiClO_4$–PC solution at the potential drops of 4.25 V_{Li/Li^+} to various lithium injection potentials. All the current transients never follow the Cottrell behaviour, viz. there is no linear relationship between logarithmic current and logarithmic time with a slope of −0.5 in the early stage. Moreover, the initial current level at 5 s, I_{ini}, of the current transient experimentally measured is

[1] Upon discharging the cell by application of cathodic current, the lithium intercalation occurs into the $Li_{1-\delta}Mn_2O_4$ electrode.

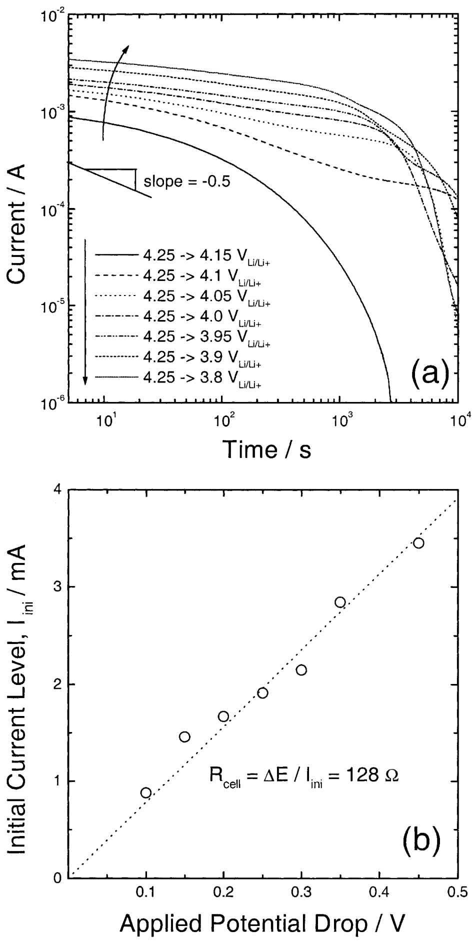

Fig. 2. (a) Cathodic current transients on a logarithmic scale experimentally measured on the $Li_{1-\delta}Mn_2O_4$ electrode in a 1 M $LiClO_4$–PC solution at the potential drops of 4.25 V_{Li/Li^+} to various lithium injection potentials, and (b) the plot of the initial current level at 5 s, I_{ini}, against the applied potential drop ΔE.

much smaller in value than that I_{ini} theoretically calculated under the 'diffusion-controlled' lithium transport. In Fig. 2(b), it was also found that I_{ini} is linearly proportional to the applied potential drop, ΔE, indicating that the relationship between I_{ini} and ΔE just follows Ohm's law.

In our previous works [13–15], both the non-Cottrell behaviour of the current transient and the Ohmic relationship between the initial current level and the applied potential drop are responsible for the 'cell-impedance controlled' lithium transport. The 'cell-impedance' means the internal cell resistance, major sources of which may be the bulk electrolyte, electrolyte/electrode interface, and bulk electrode [18]. Therefore, in the present work, it seems to be reasonable to assume that lithium transport through the $Li_{1-\delta}Mn_2O_4$ electrode proceeds under the 'cell-impedance controlled' constraint.

Under the circumstances, we theoretically simulated the current transient based upon the assumption of the purely 'cell-impedance controlled' lithium transport. The individual particle of the cubic-spinel $LiMn_2O_4$ in the composite electrode is almost spherical in shape and lithium ions diffuse zigzag through the three-dimensional diffusion path of the tetragonal 8(a) and octahedral 16(c) sites. Therefore, for the analysis of lithium transport through the electrode, we take the spherical symmetry of these oxide particles into account.

The governing equation in this case is the Fick's diffusion equation for sphere. The initial condition (IC) and the impermeable boundary condition (BC) are also given as

$$\text{IC}: \quad c = c_0, \quad \text{for } 0 \le r \le R^* \text{ at } t = 0 \tag{1}$$

$$\text{BC}: \quad zFA_{ea}\tilde{D}_{Li^+}\left(\frac{\partial c}{\partial r}\right) = 0, \quad \text{for } r = 0 \text{ at } t \ge 0 \tag{2}$$

where c and c_0 are the local and the initial concentration of lithium ion, z the valence number, F the Faraday constant, A_{ea} the electrochemical active area, $\tilde{D}_{Li^+}$ the chemical diffusivity of lithium ion, r the distance from the centre of the oxide particle and R^* represents the average radius of the oxide particle. In addition, the 'cell-impedance controlled' constraint is written as [13–15]

$$\text{BC}: \quad zFA_{ea}\tilde{D}_{Li^+}\left(\frac{\partial c}{\partial r}\right) = \frac{|E - E_{app}|}{R_{cell}}, \quad \text{for } r = R^* \text{ at } t > 0 \tag{3}$$

where E_{app} is the applied potential and R_{cell} represents the 'cell-impedance'.

In the process of numerical simulation, the 'cell-impedance' R_{cell} was determined to be ca. 128 Ω from Fig. 2(b), and the average radius of the oxide particle R^* was estimated to be ca. 1 μm from scanning electron microscopy (SEM). For the sake of simplicity, we set the electrochemical active area A_{ea} at the total surface area of the oxide particles for the composite electrode composed of the spherical particles. In the present work, A_{ea} was evaluated to be ca. 9.8 cm^2 from the pure mass of the oxide in the composite electrode and the theoretical density of the oxide.

Noticeably, in our previous work [8] on the theoretical analysis of the chemical diffusivity of lithium ion in the $Li_{1-\delta}Mn_2O_4$ electrode, it was reported that the chemical diffusion of lithium ion in the ordered phase region is strongly enhanced due to locally disturbed ordering of lithium ion. Therefore, we are necessitated to consider the variation of the chemical diffusivity of lithium ion with lithium content for the analysis of lithium transport involving the ordering of lithium ion. Fig. 3 depicts the chemical diffusivity of lithium ion experimentally determined at various lithium contents by using the measured potential transient and coulometric titration curve from GITT [8]. The functional expression $\tilde{D}_{Li^+} = f(1-\delta)$ for the variation of the chemical diffusivity with lithium content was obtained by polynomial regression analysis of the plot in Fig. 3.

Fig. 4 demonstrates the current transients calculated from the numerical solution to the Fick's diffusion equation for the conditions of Eqs. (1)–(3) at various applied potential

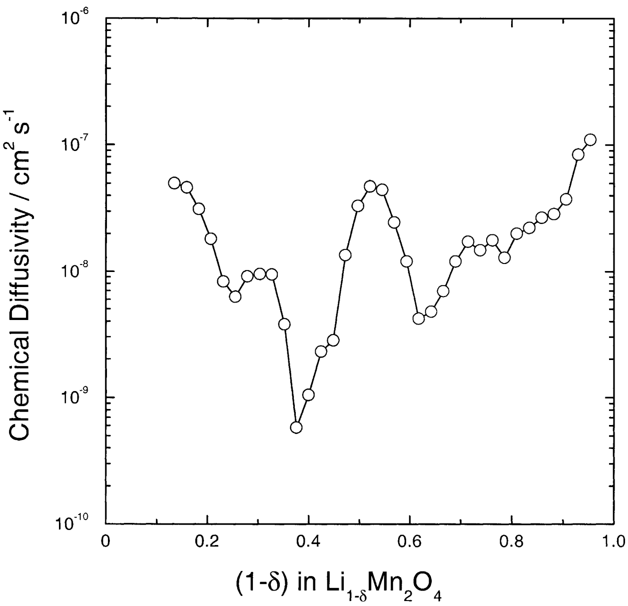

Fig. 3. Plot of the chemical diffusivity of lithium ion $\tilde{D}_{Li^+}$ on a logarithmic scale against lithium content $(1-\delta)$, experimentally determined by using the measured potential transient and coulometric titration curve from GITT [8].

drops. The theoretical current transients were in good agreement as a whole with the measured current transients (Fig. 2(a)) in value and shape. The slight discrepancy between the current transients theoretically calculated and experimentally measured is mainly attributable to the size distribution of the oxide particles in the composite electrode [19].

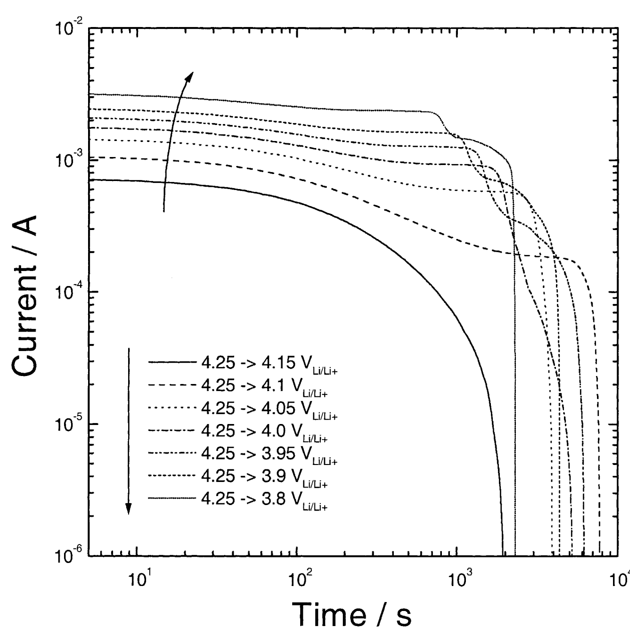

Fig. 4. Cathodic current transients numerically calculated at the potential drops of 4.25 V_{Li/Li^+} to various lithium injection potentials, based upon the 'cell-impedance controlled' constraint at the interface between electrolyte and electrode of spherical symmetry, and the impermeable constraint at the centre of the spherical oxide particle.

In order to elucidate the effect of the ordering of lithium ion on lithium transport in detail, the current transients were categorised according to the condition of the applied potential drop. The first one is the current transient obtained at the applied potential higher in value than the disorder to order transition point of ca. 4.13 V_{Li/Li^+} (Fig. 1(b)). From the electrode potential versus lithium content curve (Fig. 1(a)), it can be expected that lithium content of the electrode would change within the single disordered phase region as the initial potential 4.25 V_{Li/Li^+} is dropped to a lithium injection potential 4.15 V_{Li/Li^+}. In this case, both current transients theoretically calculated and experimentally measured alike showed a monotonic increase of its slope in absolute value during the lithium intercalation.

The second one is the current transient obtained at the potential step that encounters the disorder to order transition point of ca. 4.13 V_{Li/Li^+}, i.e. at the potential drops of 4.25–4.05 and 4.1 V_{Li/Li^+}. As time went on from $t = 0$, the logarithmic currents decreased first slowly, then remained nearly constant and finally decayed steeply with logarithmic time. It should be stressed that the appearance of the 'quasi-current plateau' in the second stage of the current transient is very similar to that appearance of the current transients measured on the $Li_{1-\delta}CoO_2$ [13,14], $Li_{1+\delta}[Ti_{5/3}Li_{1/3}]O_4$ [15], $Li_{1-\delta}NiO_2$ [15] and $Li_\delta V_2O_5$ [15] electrodes as the lithium intercalation is accompanied by the phase transformation of the lithium-poor α-phase to the lithium-rich β-phase.

The final one is the current transient obtained at the potential step that encounters both the disorder to order and the order to disorder transition points of ca. 4.13 and 4.01 V_{Li/Li^+}, respectively, i.e. at the potential drops of 4.25–3.8, 3.9 and 3.95 V_{Li/Li^+}. In this case, the current transients exhibited two 'quasi-current plateaux'. The typical current transients showing the 'quasi-current plateau' theoretically calculated are plotted on a logarithmic scale along with the corresponding variation of lithium content in the electrode with logarithmic time in Fig. 5(a).

From the comparison between the typical current transient and the corresponding variation of lithium content with logarithmic time, it can be expected that the transition of the disordered phase to ordered phase occurs within the composition interval between the onset (○) and end (●) of the first 'quasi-current plateau'. Similarly, the transition of the ordered to disordered phase takes place within the composition interval between the onset (△) and end (▲) of the second 'quasi-current plateau'. Moreover, the current transient exhibited a steep current drop in value within the time interval between the end (●) of the first 'quasi-current plateau' and the onset (△) of the second 'quasi-current plateau'.

Fig. 5(b) envisages the concentration profile across the electrode each time interval of 20 s, numerically calculated at the potential drop of 4.25–3.8 V_{Li/Li^+}. It is easily seen that

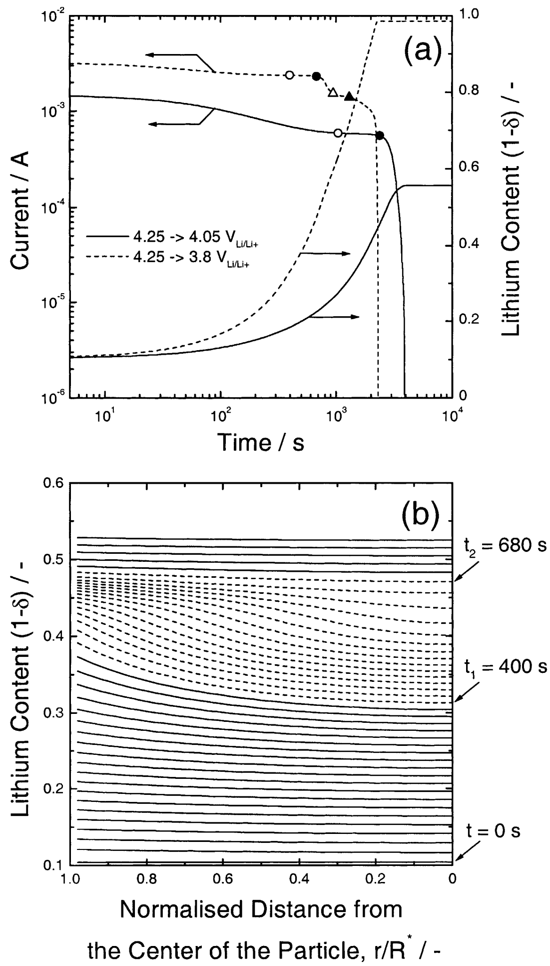

Fig. 5. (a) Typical cathodic current transients and the corresponding variation of lithium content in the electrode, numerically calculated at the potential drops of 4.25–4.05 and 3.8 V_{Li/Li^+}, and (b) the concentration profile across the electrode each time interval of 20 s, numerically calculated at the potential drop of 4.25–3.8 V_{Li/Li^+}. The open (○) and closed circles (●) indicate the onset and end of the first 'quasi-current plateau', respectively, and the open (△) and closed triangles (▲) represent the onset and end of the second 'quasi-current plateau' in the current transient, respectively.

lithium ions undergo the 'apparent' potentiostatic boundary condition rather than the 'real' potentiostatic boundary condition at the electrolyte/electrode interface [13]. In particular, the concentration profiles in the range of $t_1 \leq t \leq t_2$, indicated by dashed lines, showed an inflexion point, as compared with those concentration profiles at $t < t_1$ and $t > t_2$.

As shown in Fig. 3, the chemical diffusivity of lithium ion decreases exponentially with increasing lithium content $(1 - \delta)$ up to ca. 0.38 in the disordered phase region, and then increases abruptly with $(1 - \delta)$ up to ca. 0.5 in the ordered phase region. The combination of Figs. 3 and 5(b) indicates that the local change occurs in the chemical diffusivity of lithium ion near the transition composition of the disordered to ordered phase in the range $0.38 \leq (1 - \delta) \leq 0.5$ in average and $400\ \mathrm{s} \leq t \leq 680\ \mathrm{s}$. This local change in $\tilde{D}_{Li^+}$ may lead to the local change in the concentration gradient of lithium ion in the electrode under the 'apparent' potentiostatic boundary condition. From the above consideration, the appearance of the inflexion point in the concentration profile indicates strongly the coexistence of the disordered and ordered phases in the electrode under the 'apparent' potentiostatic boundary condition.

In addition, the values of t_1 and t_2 which were determined from the appearance of the inflexion point in the concentration profile (Fig. 5(b)) well coincided with those values of time corresponding to the onset (○) and end (●) of the first 'quasi-current plateau' in the current transient (Fig. 5(a)). The coincidence between those values of time was also found for the second 'quasi-current plateau' in the current transient.

From the results, it is suggested that two 'quasi-current plateaux' in the current transients at the potential drops of 4.25–3.8, 3.9 and 3.95 V_{Li/Li^+} are ascribed to the coexistence of the disordered and ordered phases: the first 'quasi-current plateau' indicates the coexistence of the disordered phase (lithium-poor phase) and the ordered phase, and the second 'quasi-current plateau' means the coexistence of the ordered phase and the disordered phase (lithium-rich phase). The steep current drop in value with logarithmic time between two 'quasi-current plateaux' is mainly attributable to the steep potential drop by the ordering of lithium ion at $(1 - \delta) = 0.5$; this means the abrupt decrease in the driving force for lithium transport according to Eq. (3).

Our result supports the 'three-phase model' Yang et al. [20] suggested recently for the lithium-excess cubic-spinel. From in situ synchrotron X-ray diffraction, they suggested the coexistence of the phase III (lithium-poor phase) and the phase II in the range of ca. $0.06 < (1 - \delta) < 0.44$, and the coexistence of the phase II and the phase I (lithium-rich phase) in the range of ca. $0.55 < (1 - \delta) < 0.95$. Those results are not consistent with the previous result of X-ray diffraction reported by Ohzuku et al. [21] that a single cubic phase is present in the range of ca. $0.6 < (1 - \delta) < 1$. On the other hand, Abiko et al. [5] reported the coexistence of two phases in the range of ca. $0.54 < (1 - \delta) < 0.68$ and ca. $0.76 < (1 - \delta) < 0.91$ for the stoichiometric cubic-spinel, due to the appearance of a new phase at about $(1 - \delta) = 0.7$ below 278 K. Owing to inconsistencies among Yang et al. [20], Ohzuku et al. [21] and Abiko et al. [5], further structural studies on the stoichiometric and defect cubic-spinel lithium manganese oxides at various temperatures are strongly needed for more detailed assessment of lithium transport as a function of lithium content $(1 - \delta)$ above 0.5.

In conclusion, lithium transport through the $Li_{1-\delta}Mn_2O_4$ electrode is governed by the 'cell-impedance controlled' constraint during the whole lithium intercalation involving the disorder to order transition. During 'cell-impedance controlled' lithium transport through the disordered phase, the ordered phase forms just beneath the surface of the oxide particle, and then slowly grows toward the centre of the oxide particle under the 'apparent' potentiostatic boundary condition.

Acknowledgements

The receipt of research grant under the programme 'Development of Cathode Material in Rechargeable Lithium Battery for High Efficient Energy Reservoir 1999/2000' from the Electrical Engineering and Science Research Institute (EESRI), Korea is gratefully acknowledged. Incidentally, this work was partly supported by the Brain Korea 21 project.

References

[1] M.M. Thackeray, Prog. Solid State Chem. 25 (1997) 1.
[2] R.J. Gummow, M.M. Thackeray, J. Electrochem. Soc. 141 (1994) 1178.
[3] Y. Gao, J.N. Reimers, J.R. Dahn, Phys. Rev. B 54 (1996) 3878.
[4] T. Kudo, M. Hibino, Electrochim. Acta 43 (1998) 781.
[5] H. Abiko, M. Hibino, T. Kudo, Electrochem. Solid State Lett. 1 (1998) 114.
[6] R. Darling, J. Newman, J. Electrochem. Soc. 146 (1999) 3765.
[7] S.-I. Pyun, S.-W. Kim, Mol. Cryst. Liq. Cryst. 341 (2000) 155.
[8] S.-W. Kim, S.-I. Pyun, Electrochim. Acta 46 (2001) 987.
[9] J.R. Dahn, W.R. McKinnon, J. Phys. C 17 (1984) 4231.
[10] J.N. Reimers, J.R. Dahn, J. Electrochem. Soc. 139 (1992) 2091.
[11] A. Van der Ven, M.K. Aydinol, G. Ceder, G. Kresse, J. Hafner, Phys. Rev. B 58 (1998) 2975.
[12] M.Y. Saïdi, J. Barker, R. Koksbang, J. Solid State Chem. 122 (1996) 195.
[13] H.-C. Shin, S.-I. Pyun, Electrochim. Acta 45 (1999) 489.
[14] S.-I. Pyun, H.-C. Shin, Mol. Cryst. Liq. Cryst. 341 (2000) 147.
[15] H.-C. Shin, S.-I. Pyun, S.-W. Kim, M.-H. Lee, Electrochim. Acta 46 (2001) 897.
[16] S.-I. Pyun, Y.-M. Choi, I.-D. Jeng, J. Power Sources 68 (1997) 593.
[17] K. Binder, D.P. Landau, Phys. Rev. B 21 (1980) 1941.
[18] M.G.S.R. Thomas, P.G. Bruce, J.B. Goodenough, J. Electrochem. Soc. 132 (1985) 1521.
[19] H.-C. Shin, S.-I. Pyun, Electrochim. Acta 44 (1999) 2235.
[20] X.Q. Yang, X. Sun, S.J. Lee, J. McBreen, S. Mukerjee, M.L. Daroux, X.K. Xing, Electrochem. Solid State Lett. 2 (1999) 157.
[21] T. Ohzuku, M. Kitagawa, T. Hirai, J. Electrochem. Soc. 137 (1990) 769.